Ain Shams Engineering Journal 14 (2023) 102217

Contents lists available at ScienceDirect

Ain Shams Engineering Journal

journal homepage: www.sciencedirect.com

Using oxy-hydrogen gas to enhance efficacy and reduce emissions of diesel engine

Mohamed F. Al-Dawody [a], Khaled A. Al-Farhany [a], Shrok Allami [b], Kadhim K. Idan Al-Chlaihawi [a], Wasim Jamshed [c,*], Mohamed R. Eid [d,e], Aeshah A. Raezah [f], Ayesha Amjad [g,h], Sayed M. El Din [i]

[a] Department of Mechanical Engineering, University of Al-Qadisiyah, Al-Qadisiyah 58001, Iraq
[b] Ministry of Science and Technology/Renewable Energy Directory, Iraq
[c] Department of Mathematics, Capital University of Science and Technology (CUST), Islamabad 44000, Pakistan
[d] Department of Mathematics, Faculty of Science, New Valley University, Al-Kharga, Al-Wadi Al-Gadid 72511, Egypt
[e] Department of Mathematics, Faculty of Science, Northern Border University, Arar 1321, Saudi Arabia
[f] Department of Mathematics, Faculty of Science, King Khalid University, Abha 62529, Saudi Arabia
[g] Faculty of Organization & Management, Silesian University of Technology, 44-100 Gliwice, Poland
[h] Centre for Mechanical Engineering, Materials and Processes (CEMMPRE) University of Coimbra, Polo II, Coimbra, 3030-788, Portugal
[i] Center of Research, Faculty of Engineering, Future University in Egypt, New Cairo 11835, Egypt

ARTICLE INFO

Article history:
Received 19 October 2022
Revised 1 February 2023
Accepted 23 February 2023
Available online 03 March 2023

Keywords:
Oxy-hydrogen gas
Diesel engine fuel
Diesel combustion model
Pollutant emissions

ABSTRACT

The ever-increasing need for energy, along with diminishing petroleum supplies, has prompted the quest for renewable and sustainable alternative fuels. The goal of this research is to investigate theoretically the impact of using HHO gas on single-cylinder diesel engine characteristics using the simulation software diesel-RK model. Diesel fuel blended with 10% HHO gas is used and tested under different engine speeds. When 10% HHO gas was put into the engine, the thermal efficiency climbed to 31.5 percent and consequently, fuel consumption is reduced by up to 20 percent. The maximum reduction in BSN is 25% which is witnessed at 3500 rpm. The findings are corroborated by the findings of other studies. Among the most important outcomes that were obtained the peak combustion pressure was raised by 10% as compared to diesel fuel without HHO and the brake power enhances from (9% to 16%) when the engine speed is increased from (1500 to 3500) rpm.

1. Introduction

1.1. Motivation

Growing energy demand, hazardous pollutants, and oil shortages all led to the hunt for a cost-effective alternative fuel. Petroleum fuels play a pivotal role in this kind of advance in order to expand main industries such as agriculture, transportation, and industry, as well as to fulfill other significant human requirements [1]. Advancement of diesel injection time is a viable strategy to reduce unburned methane and green house gas emission of natural gas or diesel dual-fuel engines at reduced engine loads, according to prior study. Under circumstances of medium to high load-low speed, this improvement could not last though. Every year, around 11,000 million tons of fossil fuels are utilized worldwide. Such usage would quickly deplete the resources. As demand for energy rises, so does the environmental effect of its expansion. As diesel fuel, vegetable oils (castor oil, cottonseed oil, Jatropha, etc.) offer low sulfur, high flash, and lubricity. Their main drawbacks are their extremely high viscid and decreased cetane level, calorific value, and volatility [2]. Despite cotton ethyl ester having a lower calorie content, low sulfur level, and higher moisture absorption than crude petroleum, it has worse thermal performance, output power, and higher volumetric efficiency. Because of the oxygen levels and cetane number of biodiesel, CO emissions decreased while NOx emissions increased when compared to fossil diesel. Increasing environmental pollution and depletion of fossil fuels have necessitated a strong interest in the research of alternative fuel sources. Air pollution is not only considered a nuisance, but also a threat to public health. In general, air pollution has a detrimental impact

* Corresponding author.
E-mail addresses: Mohamed.Aldawody@qu.edu.iq (M.F. Al-Dawody), Khaled.alfarhany@qu.edu.iq (K.A. Al-Farhany), kadhim.idan@qu.edu.iq (K.K. Idan Al-Chlaihawi), wasiktk@hotmail.com (W. Jamshed), mreid@scinv.au.edu.eg (M.R. Eid), Aalraezh@kku.edu.sa (A.A. Raezah), Ayesha.amjad@polsl.pl (A. Amjad), sayed.eldin22@fue.edu.eg (S.M. El Din).

https://doi.org/10.1016/j.asej.2023.102217
2090-4479/

Nomenclature

A_0, A_1, A_2, A_3	constants	p_s	fuel saturating vapor pressure
BSN	Bosch smoke number	PM	particulate material
BSFC	brake specific fuel consuming	rpm	revolutions/minute
$[C]$	cylinder concentricity soot	rps	revolutions/second
°C	degrees centigrade	T	temperature in the cylinder
°CA	crank angle degrees	t	time
CN	cetane number of fuel	TDC	top dead center
DF	diesel fuel	V	instantaneous fuel velocity
l	spraying length	V_0	spray Initial velocity
lm	penetrable distance	V_m	velocity of the spray's front
m_f	fuel mass	V_c	cylindrical volume
NOx	nitrogen oxides	x	heat release proportion
p	cylinder pressure (Pa)	x_0	fuel fractional vapor formed in delay period

on people's health, drives up living expenses, damages the environment, and hurts the economy. Additionally, traditional fuels made of petroleum have a finite amount of resources. Another issue is the daily rise in gasoline prices brought on by the dearth of petroleum supplies. As a result, researchers and engine manufacturers are under pressure to come up with a fresh plan for increasing fuel economy and reducing emissions from internal combustion engines.

1.2. Literature review

Survey [3] demonstrated the engine efficiency and fuel properties while utilizing biofuels and alcohol as renewable fuels. The impacts of alternative fuels on emission characteristics including NOx, CO, and HC are also described. A single cylinder diesel engine is being tested with Gas-to-Liquid (GTL) and an ethanol-RME-Diesel combination as alternative fuels [4]. Combustion engines that run on acetylene have had their efficiency, emissions, and combustors investigations thoroughly reviewed. It has been determined that these engines can run on acetylene without undergoing significant changes in [5]. Therefore, an increase in interest in low-carbon alternative fuels is adopted. Energy-efficient, available, high octane number, powerful flame speed, greater heating value than fossil fuels, and low-polluting are among the factors that made hydrogen (H_2) the best candidate for fossil fuels [6,7]. However, the difficulty of liquefaction and the prevention of leaks made the storage of pure hydrogen extremely difficult and dangerous which increased the cost of hydrogen to be used as fuel in IC engines [8]. Therefore, the most commonly applicable way to bring hydrogen and IC engines together is the electrolysis of pure water through an HHO system [9]. The HHO, also known as Brown's gas, is a gaseous fuel produced from the electrolysis of pure water and consists of a combination of hydrogen (66.7%) and oxygen (33.3%) gases. HHO is completely safe, eco-friendly, has high fire spread rates, and has high specific energy per unit weight, Because of its oxygen component, it has superior combustion properties to pure hydrogen, and has much more flammability compared to diesel [10,11]. The higher calorific value of hydrogen content in HHO gas led to the introduction of HHO to improve the engine output brake power from 5.07 to 11.5% [12,13]. Moreover, the impacts of hydrogen and oxygen content on complete combustion improve thermal efficiency and decrease specific fuel consumption by 6 to 12% [14].

The understanding of HHO addition effect on IC engine was the attention of many researchers and a significant amount of work has been devoted to this field Yilmaz et al. [15] informed that the usage of HHO improved the torque of CI engine by an average of 19.1%; on the other hand, the specific fuel consumption, carbon monoxide, and hydrocarbon emissions were reduced by an average of 14%, 13.5%, and 5% respectively. Engineers working in the area of power system have focused in particular to the energy management system for homes (HEMS), which is dependent on cutting-edge intelligent devices and controls the adequacy between consumption and power supply [16,17]. Arat et al. [18] examined the impact of using Hydroxy - CNG (25% HHO-75% CNG) fuel mixtures on the performance of 3.6 L, 4- cylinders, 4-stroke diesel engine and obtained improvements of 4.75% in brake torque and 6.85% in brake power, whereas the brake specific fuel consumption (BSFC) decreased by about 27.2% compared to the neat diesel operation. EL-Kassaby et al. [19] showed that the thermal efficiency of a 1.3 GLXi Skoda Felicia gasoline engine improved by about 10%, whereas the fuel consumption, HC, CO, and NOx emissions decreased by (34, 18, 14, and 15) % respectively with the induced of HHO in the intake manifold. Gohar and Hassan [20] compared the performance characteristics of a 232 cm^3 CI engine with and without hydroxy (HHO) gas addition. They found an increment of about 22% in brake power, 47% in thermal efficiency, and 24%, in mechanical efficiency, and also they found there is a decrement of 35% in BSFC. Matienzo [21] performed experimentation on a 930 CC diesel engine and reported that with the addition of HHO With an average of 3.81 percent and 2.79 percent improvement in BSFC and thermal efficiency, also the engine vibrations level was reduced HHO. Rimkus et al. [22] noticed that the addition of HHO has an adverse effect on the performance of the 1896CC −4 cylinders CI engine where the brake torque decreased by 2.6% and specific fuel consumption increased by 2%. This can be attributed to the pre-ignition of the fuel mixture at the end of compression due to the presence of small fractions of monoatomic hydrogen and oxygen which ignite spontaneously before the autoignition temperature of the fuel mixture was achieved. Nabil [23] performed experiments on two engines; 150CC and 1300CC and found a reduction in fuel consumption by about 14.8 % and 16.3 % for the two engines through the addition of HHO. Also, a reduction in CO of about 33 % and 24.5 %, as well as a reduction in HC emission gases of about 27.4 % and 21 % were found for the two engines respectively. Kazim et al. [24] scrutinized the influences of the addition of HHO on a 315CC- CI engine performance and recorded a maximum enhancement in engine performance where torque and power both increased by 22.4 percent. Moreover a 19.4% increase in efficiency with 10 ft^3/hr flow rates of HHO. Najafi et al. [25] indicated that the introduced HHO at a flow rate of 5CC/s as a low-level gaseous additive via the inlet multifarious of a single-cylinder, constant speed, the dual-fueled diesel engine can enhance break power by about 2.5% compared with

Diesel fuel. Moreover, the brake-specific fuel consuming, CO_2, and CO emissions decreased by around 11%, 7 %, and 6 % associated with diesel, correspondingly. Dahake et al. [26] compared the performance of the VCR engine with a constant flow of hydroxyl (HHO) gas in the intake manifold and with the baseline diesel fuel. They indicated a maximum performance improvement at 18 CR, where the BTE increased by 9.25 percent, BSFC diminished by 15%, HC emissions reduced, and CO emissions reduced by 23% at full load conditions respectively.

1.3. Novelty

Extensive experimental research works have been carried out to find alternate fuels for internal combustion (IC) engines, with a distinct absence of numerical investigation. In this work, a computational reproduction by the diesel-RK program was used to estimate the effect of inducing 10% HHO to diesel on the performance, emissions, and combustion characteristics of diesel engines running at diverse speeds. The purpose of this study is to use the simulation program diesel-RK model to theoretically analyze the effects of employing HHO gas on single-cylinder diesel engine characteristics.

2. Theoretical analysis

2.1. Fundamental HHO technology

The HHO technology is defined as a system that is connected to a sparking ignition or compression ignition engine and delivers a stoichiometric hydroxide mixture known as HHO gas to the intake system [19,27]. Electrolysis is the furthermost public process utilized to split H_2 from H_2O under applied power, using a unique cell design consisting of an anode and cathode inside aqueous conductive media. The basics of water splitting are explained by the following equations.

$$2H_2O + 2e^- \rightarrow H_2 + 2OH \text{ (Cathode)} \quad (1)$$

$$2OH \rightarrow H_2O + \frac{1}{2}O_2 + 2e^- \text{ (Anode)} \quad (2)$$

$$H_2O + 286kJ \rightarrow H_2 + \frac{1}{2}O_2 \text{ (Total)} \quad (3)$$

Fig. 1 shows the HHO generator diagram. It comprises a water supply tank (1) that provides a steady water flow to the HHO cell (2) to prevent the cell from overheating and to supply hydrogen generation continuously. A separator tank (3) is used to separate water droplets from HHO, eliminate the introduction of electrolytes and water into the induction system of the IC engine, and return them to the bottom of the HHO cell. The engine intake manifold is fed with hydrogen and oxygen gases. Safety valve on separator tank used to control the pressure inside HHO generator. Bubbler (4) is also used after the separation tank as a flame arrestor. To calculate the HHO gas generation rate, the gas goes into the open pool of water, causing the water to drop down from the inverted graded cylinder after leaving the separation tank. The amount of water over time was utilized to calculate the HHO flowing rate. HHO flow rate was calculated as the accumulated cylinder gas volume per time. The cell productivity is computed from the equation below (4):

$$HHO_{productivity} \rightarrow \frac{Volume}{time} \quad (4)$$

The electrolysis cell in the HHO generator constructed from the electrode stack consists of two types of electrodes, anode, and cathode. The anode and cathode are placed sequentially with a

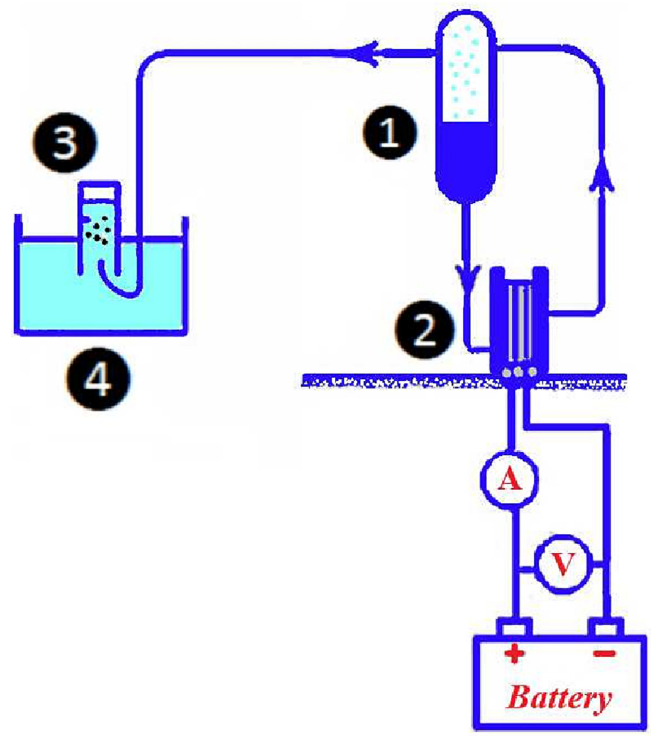

Fig. 1. Generating system of the HHO gas [19].

gap of 3 mm between them. HHO gas production primarily depends on the gap between these electrodes, directly proportional to the surface area of the anode and cathode electrodes, the type and concentration of the aqueous solution, and the voltage difference between the anode and cathode electrodes applied. When an electrical potential is applied between the electrolyzer's electrodes, HHO gas is directly transported. There are two kinds of HHO cells: dry and wet. In this work, HHO-dried cell is considered.

In contrast to a wet cell, a dry structure produces no free liquid and may function in any direction without leaking, which makes it suitable for lifting devices. As opposed to the early wet cells, which were often delicate glass jars with lead rods dangling from the open top, they required to be handled carefully to prevent spills. There are many advantages of the dried cell compared to the wetted cell for HHO production. Wet cells are less dependable and suited than dry cells. The electric connection in the wet cell corroded severely due to direct exposure to the electrolyte that needs maintenance, increase cost, and reduced production. The dry cell's safety characteristics are more hopeful than the wet cells., since starting the cell works by sparking the connections under the electrolyte exposure.

2.2. HHO cell (Dry)

The electrodes were steel (stainless) tumbler plates. The electrodes are $16 \times 20 \times 0.2$ cm thick, and they are arranged as indicated in Fig. 2, where $(+, -, N)$ denote positive, negative, and neutral electrodes respectively. The current goes from the negative battery connection to the positive terminal via the neutral plates. For HHO production, neutrals decrease the plate's voltage and enhance the surface area. Rubber gaskets were used to keep the space between neighboring tumblers to 1 mm. In addition, acrylic cover plates measuring $20 \times 24 \times 1$ cm in thickness were produced to provide a visual indicator of electrolyte level. The engine's bat-

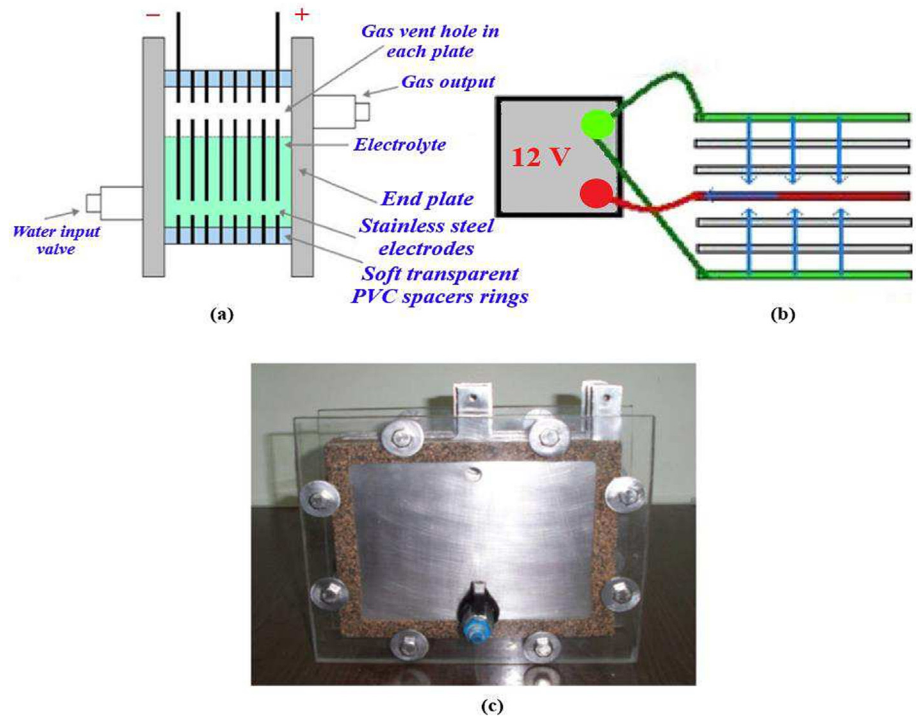

Fig. 2. (a) Schematic diagram of HHO cell, (b) Arrangement of 2-neutral plates, and (c) Real dry cell [19].

tery supplies electrical energy to the HHO cell, which is then recharged by the alternator. The calculation is done based on the following equations mentioned in [19]:

$$m_{H2} = \frac{V_h}{V_{kmol}} M_w. \tag{5}$$

Where V_h is the volume of collected hydrogen = 0.11 cylinder's volume; $V/kmole$: occupied volume per 1 $kmol = 0.224 * 10^2 m^3$; M_w signifies hydrogen's molecular weight

$$\text{Gained energy} = m_{H2} * LCV_{H2} \tag{6}$$

$$\text{Energy consumption} = V.A.T \tag{7}$$

$$\eta_{HHO} = \frac{\text{Gained energy}}{\text{Energy consumption}} \tag{8}$$

3. Numerical analysis

The numerical simulation is done with the aid of Diesel-RK software and is used to examine the performance, emissions, and combustion characteristics of a single-cylinder, 4-stroke, DI diesel engine powered by 10% HHO + 90% Diesel [28,29]. The details of the individual equations used in the simulation are taken from [30–32].

The numerical analysis is performed on a single-cylinder diesel engine. Table 1 displays the engine's specifications. All the calculations were carried out under full load with constant compression ratio and variable engine speed ranges from (1500–3500) rpm. 10% of HHO gas is inducted theoretically with air in the induction system. The properties of diesel and HHO gas are listed in Table 2.

The properties of HHO gas are admitted to the software's fuel library along with the properties of diesel fuel.

Table 1
Engine dimensions [28].

Engine Brand	Kirloskar TAF-1
Type of engine	4-Stroke, Diesel Engine
Bore	80 mm
stroke	110 mm
The cylinder capacity	0.553 L
The compression ratio	15.5
Rated power	3.7 kW, 1500 rpm
Orifice diameter	0.15 mm
Injection pressure	220 bar

Table 2
Physiochemical properties of fuels under investigation.

Property	Diesel	HHO	10%HHO
C%	87	0	78.30
H%	12.6	100	21.34
O%	0.004	0	0.0036
Density (kg/m^3)	830	83.764	755.37
Viscosity (cst)	3.0	0.009	2.701
Calorific value (MJ/kg)	42.5	120,000	50.25
Flash point (°C)	76	–	68.4
Cetane number	48	53.3	48.53
Molecular weight	190	2	171.2

3.1. Spraying paradigm

Equation (1) illustrates the velocity of an elementary fuel mass (EFM) that is transported among the injector and targeted to the spraying nozzle in a microsecond time unit, as shown below

$$\left[\frac{U}{U_0}\right]^{\frac{3}{2}} = 1 - l/l_m \tag{9}$$

The history of spray evolution is illustrated in Fig. 3.

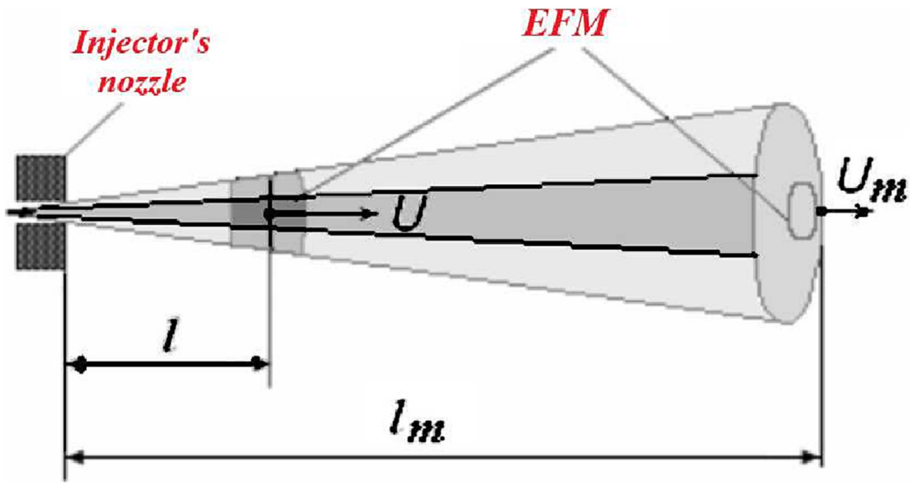

Fig. 3. Spray development v/s time [28].

3.2. Heat releasing paradigm

The burning procedure is separated into four stages, each with its characteristics that restrict the burn-up rate. The stages are listed underneath:

1. Inflammation lateness:

$$\tau = \sqrt{\frac{T}{P}} \cdot e^{\left(\frac{Ea}{8.312T} - \frac{70}{CN+25}\right)} \cdot 3.8 \times 10^{-6} \cdot \left(n \times 1 - 1.6 \times 10^{-4}\right) \tag{10}$$

2. Blended burning stage: (The burning of a blend of air and fuel vapor that is prepared early in the ignition delay).

$$\frac{dx}{dt} = \varphi_1\left(\frac{d\sigma_u}{d\tau}\right) + \varphi_0 \cdot \left[(\sigma_{\text{ud}} - x_0)(0.1\sigma_{\text{ud}} + x_o)A_0\left(\frac{m_f}{V_i}\right)\right] \tag{11}$$

3. Combustion diffusion (direct combustion of fuel after injection):

$$\frac{dx}{d\tau} = \varphi_2\left((\sigma_u - x)(\Phi - x) \cdot A_2\left(\frac{m_f}{V_c}\right)\right) + \varphi_1\left(\frac{d\sigma_u}{d\tau}\right) \tag{12}$$

4. Combustion tail (injection completes and combustion stops)

$$\frac{dx}{d\tau} = (1 - x)(\varepsilon_b\Phi - x) \cdot \varphi_3 K_T A_3 \tag{13}$$

φ discusses the completion of combustion in zones:

$$\phi = 1 - (A_1/\varepsilon_b\Phi - x)\frac{dx}{dt}\left\{r_v + \sum_{i=1}^{m_w}\left(r_{\text{wi}} \cdot 300 \cdot e^{\left(\frac{-16000}{2500 + r_{\text{wi}}}\right)}\right)\right\} \tag{14}$$

3.3. Performance calculations

a. Brake Thermal Efficiency (BTE)

It can be calculated easily from the equation below.

$$\text{BTE} = \text{BP}/\dot{m}_f * \text{LCV} \tag{15}$$

b. Brake Specific Fuel Consumption (BSFC)

It is determined from the equation below.

$$\text{BSFC} = \left(\frac{\dot{m}_f}{\text{BP}}\right) \times 3600 \tag{16}$$

3.4. Modeling of pollutant emissions

3.4.1. Nox formation modeling

The reaction of nitrogen oxides is:

$$N + O_2 \leftrightarrow NO + O \tag{17}$$

The reaction's rate is determined by the amount of oxygen present. The volumetric of NO concentration is calculated as follows [33]

$$\frac{d[NO]}{d\theta} = \frac{2.33 * 10^7 p \times e^{-\frac{38020}{T_Z}}[N_2]_e[O]_e\left(1 - \left([NO]/[NO]_e\right)^2\right)}{RT_Z\left(1 + (2365/T_Z) \times e^{\frac{3365}{T_Z}}.[NO]/[O_2]_e\right)} \cdot \left(\frac{1}{rps}\right) \tag{18}$$

3.4.2. Soot model

Comprehensive research on soot modelling is published in [29] The soot concentricity in the exhauster associated with regular constraints can be specified as

$$[C] = \int_{\theta_B}^{480} \frac{d[C]}{d\tau}\frac{d\theta}{6n}\left[\frac{0.1}{P}\right]^{\gamma} \tag{19}$$

The Bosch smoke number (BSN) was acquired from Hartridge's equation presented underneath [34]:

$$Hartidge = 100\left[1 - 0.9545 \times e^{(-24226[C])}\right] \tag{20}$$

The relation between PM and BSN is shown below:

$$[PM] = 565\left[ln\frac{10}{10 - Bosch}\right]^{1.206} \tag{21}$$

4. Validation

The purpose of this section is to compare some of the numerical study outcomes with those of other researchers' work under simi-

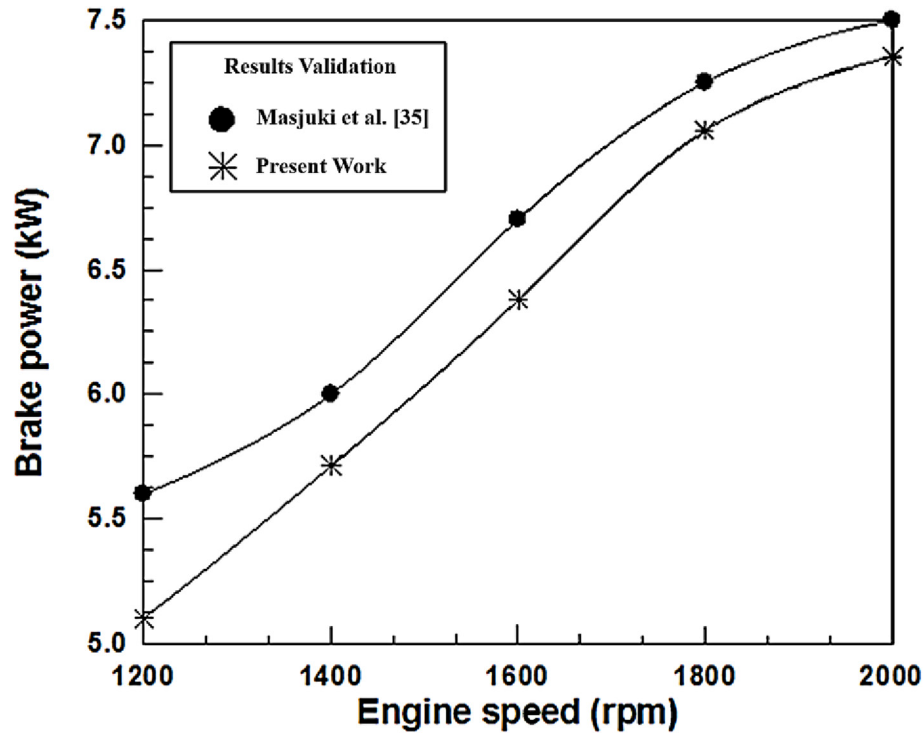

Fig. 4. Validation of brake power over various range engine speeds.

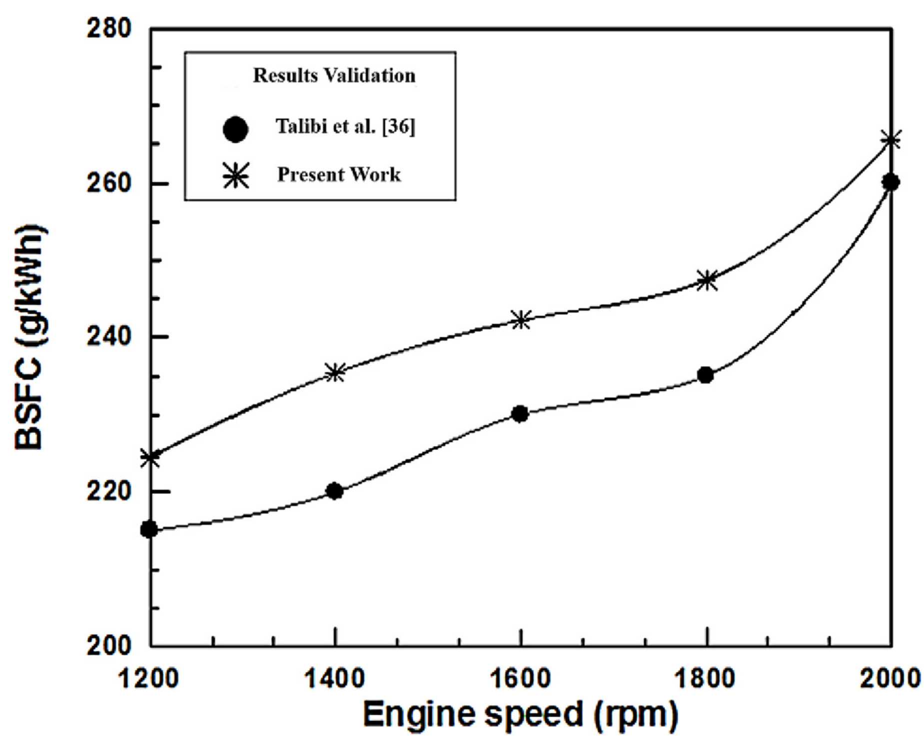

Fig. 5. Validation of BSFC over various range engine speeds.

lar operating situations. Fig. 4 explains the full load history of brake power for baseline diesel at variable speeds. It can be seen that a slight difference is detected compared to the results of Masjuki et al. [35].

Fig. 5 shows the comparison of BSFC with engine speed between the present study and the results of Talibi et al. [36]. The difference between the two is around 5%, indicating that the current study's accuracy is acceptable. The detailed validation results per engine speed listed in Table 3.

5. Simulation results

HHO gas served as a supplemental fuel in the diesel engine. A summary of test conditions is arranged in Table 4. Several variables

Table 3
Comparison of validation results for diesel.

Engine Speed (rpm)	Brake power (kW)		BSFC (g/kWh)	
	Present work	Masjuki et al. [35]	Present work	Talibi et al. [36]
1200	5.099	5.6	234	215
1400	5.710	6	245	220
1600	6.377	6.7	252	230
1800	7.057	7.25	257	235
2000	7.351	7.5	276	260

Table 4
Summary of Test conditions.

Engine Speed (pm)	% HHO	% Diesel	Injection time Diesel BTDC deg.	Compression ratio
1500	0	100	20	15.5
1500	10	90	20	15.5
2000	0	100	20	15.5
2000	10	90	20	15.5
2500	0	100	20	15.5
2500	10	90	20	15.5
3000	0	100	20	15.5
3000	10	90	20	15.5
3500	0	100	20	15.5
3500	10	90	20	15.5

Table 5
Summary of simulation results at different speeds for pure diesel fuel.

Engine Speed (rpm)	Brake power (kW)	BSFC (g/kWh)	BTE (%)	BSN	NOx (ppm)	Pmax (bar)
1500	4.90E + 00	2.51E-01	2.69E + 01	1.39E + 00	2.17E + 03	9.40E + 01
2000	6.29E + 00	2.58E-01	2.62E + 01	9.38E-01	2.59E + 03	1.02E + 02
2500	7.51E + 00	2.66E-01	2.54E + 01	7.38E-01	2.24E + 03	9.94E + 01
3000	8.23E + 00	2.83E-01	2.39E + 01	6.38E-01	1.87E + 03	9.56E + 01
3500	8.20E + 00	3.13E-01	2.16E + 01	7.03E-01	1.44E + 03	8.91E + 01

Table 6
Summary of simulation results at different speeds for 90% diesel + 10% HHO.

Engine Speed (rpm)	Brake power (kW)	BSFC (g/kWh)	BTE (%)	BSN	NOx (ppm)	Pmax (bar)
1500	5.36E + 00	2.00E-01	3.38E + 01	1.41E + 00	1.94E + 03	1.01E + 02
2000	6.94E + 00	2.04E-01	3.32E + 01	9.19E-01	2.27E + 03	1.10E + 02
2500	8.42E + 00	2.08E-01	3.26E + 01	7.03E-01	1.95E + 03	1.08E + 02
3000	9.34E + 00	2.18E-01	3.10E + 01	5.79E-01	1.64E + 03	1.04E + 02
3500	9.46E + 00	2.38E-01	2.84E + 01	5.25E-01	1.28E + 03	9.78E + 01

include performance parameters like brake power, BSFC, thermal efficiency, emission parameters such as Bosch smoke number (BSN), Nitrogen Oxides (NO_x), and also the combustion parameters such as maximum cylinder pressure are shown graphically with variable rotational speeds. All simulation results are outlines per engine speed for diesel and 10% HHO in Table 5 and 6 consequently.

Fig. 6 presents the brake power of diesel engines concerning engine speed. The power is increased from (9% to 16%) when engine speed is increased from 1500 to 3500 rpm respectively by using HHO at constant load. With higher rpm, the engine runs efficiently in comparison to the speed when HHO gas is supplied. Peak power is noticed at 3500 rpm.

As found in Fig. 7, the decrease in BSFC is due to a homogenous (air-HHO) mixture with higher HHO's diffusivity in addition to HHO gas's oxygen index that aids diesel and improves combustion. By employing 10% HHO gas, 20% reduction in BSFC is realized. Same findings are shown in the study of [37].

As seen in Fig. 8, brake thermal efficiency increases by 28% at 2550 rpm, while the incremental trend follows the same pattern where 30% increase is obtained at 3000 rpm as compared to the case without HHO.; furthermore, 31.5 percent rise was observed when the engine was accelerated to 3500 rpm. This demonstrates that when HHO gas is admitted to the engine, it works more efficiently at a constant load. The result of HHO induction on the profile of BSN is clearly seen in Fig. 9. The case of using HHO indicates a promising reduction in BSN. While the engine is operating at 1500 rpm, a 1.5% reduction is reported. The maximum reduction in BSN is 25% which is witnessed at 3500 rpm. Due to the high diffusion coefficient and increased accessibility of the fuel to oxygen, either a rise in the H/C rate of the total fuel or an increase in the homogeneity of the ignitable mixture minimizes the generation of soot emissions [38–40].

High NOx emissions are frequently accompanied by a high flame temperature and a large amount of air. When HHO is introduced into the intake manifold, the amount of diesel is reduced,

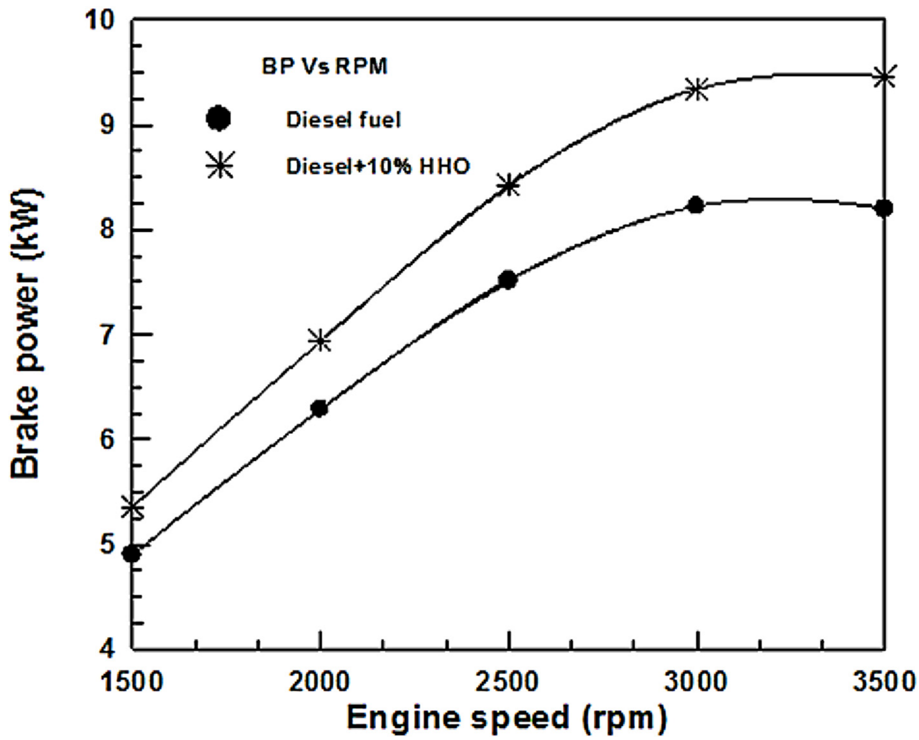

Fig. 6. Effect of engine speed on the brake power.

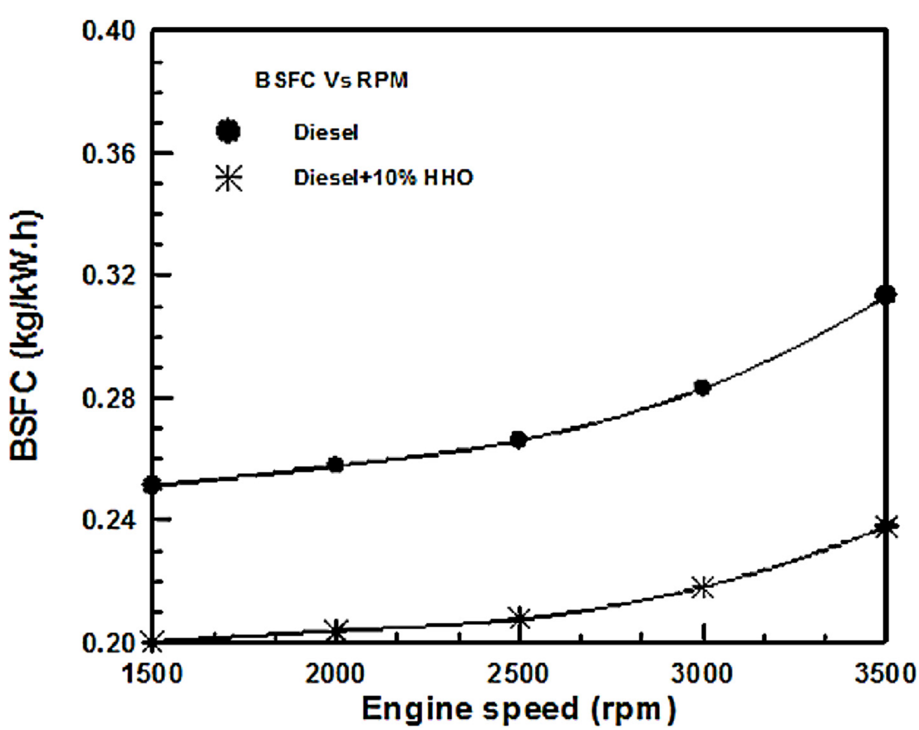

Fig. 7. Effect of engine speed on the BSFC.

resulting in a lean mixture and, as a result, a lower flame temperature. As a result, NOx decreased as seen in Fig. 10. The presence of HHO lowers emission profiles by improving combustion properties and fuel economy. The outcomes of this investigation show similar trends to those used as references [41–43].

The combustion characteristics are studied in terms of maximum pressure. It can be observed from Fig. 11 that HHO has been added along with air leading to an improvement in the rate of heat released during the power cycle which consequently increased the peak pressure in the cylinder. The rapid flame speed of hydrogen

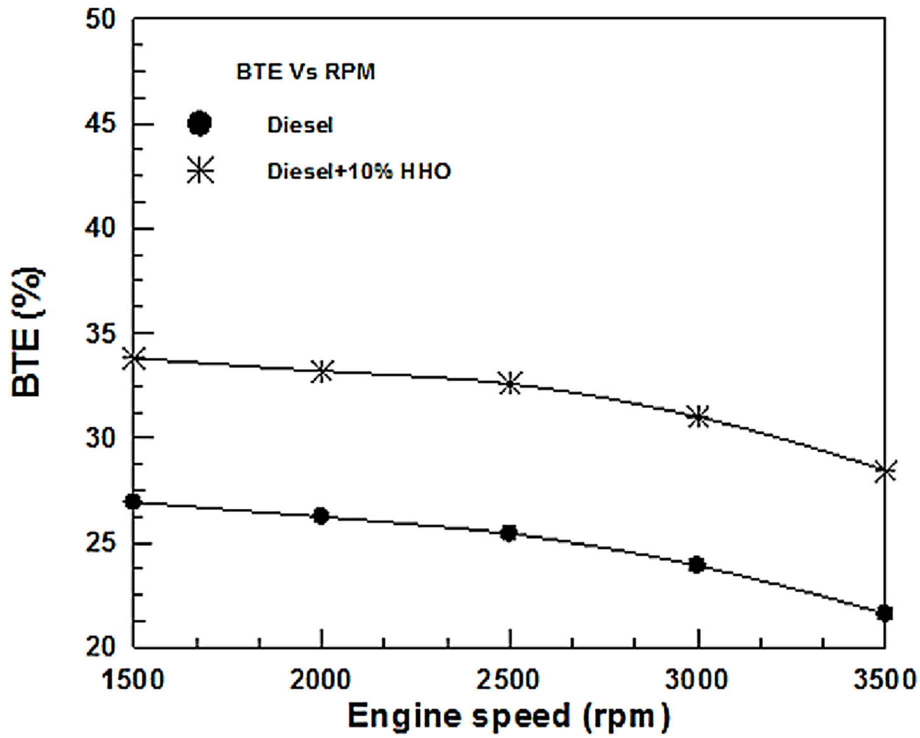

Fig. 8. Effect of engine speed on the BTE.

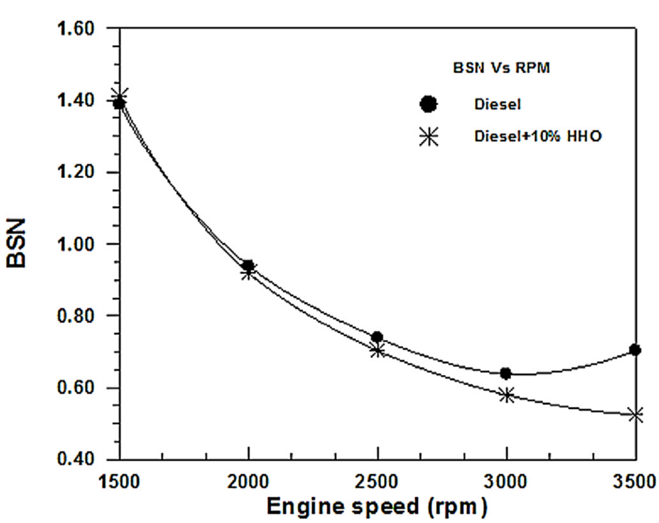

Fig. 9. Effect of engine speed on the BSN.

which is nine times faster than diesel [44] accelerates both the rate of pressure rise and the peak pressure values attained after combustion [45]. With respect to diesel feeding engine with 10% HHO at 2500 rpm, around a 9% increase in the pressure is detected, while it was 10% at 3500 rpm.

6. Conclusions

The impact of using HHO gas on single-cylinder diesel engine characteristics using the simulation software diesel-RK model has been deliberated. Diesel fuel blended with 10% HHO gas is used and tested under different engine speeds. One of the most important results reached through this careful study:

1. HHO cell is simple to integrate with the engine's system.
2. The brake power is enhanced from (9% to 16%) when the engine speed is increased from (1500 to 3500) rpm, respectively.
3. When 10% HHO gas was supplied, the engine's thermal efficiency raised to 31.5 percent.
4. Consequently, fuel consumption is reduced up to 20% as a result of admitting 10% HHO.
5. The emissions of BSN and NOx have been reduced when HHO is introduced into the system.
6. Peak combustion pressure raised by 10% as compared to diesel fuel without HHO.

Declaration of Competing Interest

The authors declare that they have no known competing financial interests or personal relationships that could have appeared to influence the work reported in this paper.

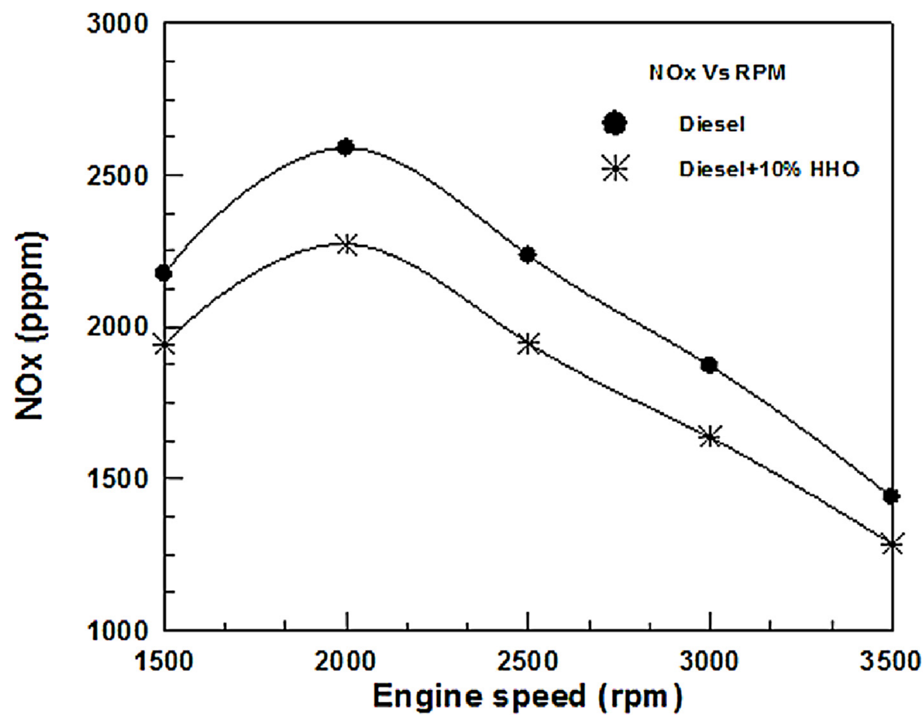

Fig. 10. Effect of engine speed on the NOx.

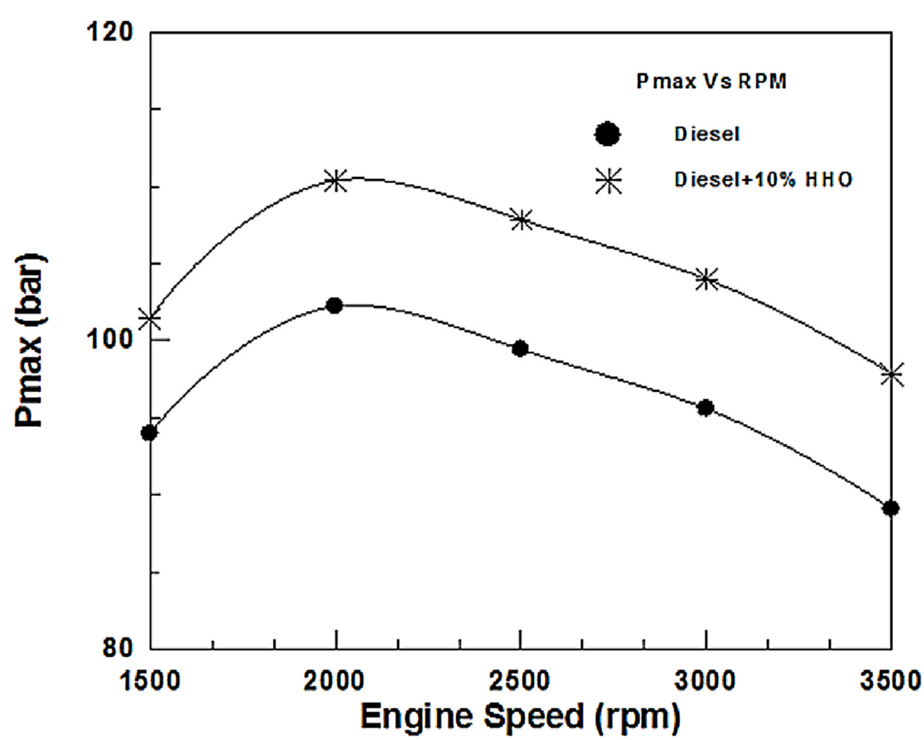

Fig. 11. Effect of engine speed on the maximum cylinder pressure.

Acknowledgments

The authors extend their appreciation to the Deanship of Scientific Research at King Khalid University, Abha, Saudi Arabia, for funding this work through the Research Group Project under Grant Number **(RGP.2/154/43)**.

References

[1] Taibani A, Visaria M, Krishnan S. A combined Combustion-Conjugate heat transfer analysis for Design of partially insulated pistons. Appl Therm Eng 2022;208:118210.

[2] Kumbhar V, Pandey A, Sonawane CR, Panchal H, Ağbulut Ü. Numerical and experimental investigation of the influence of various metal-oxide-based

nanoparticles on performance, combustion, and emissions of CI engine fuelled with tamarind seed oil methyl ester. Energy 2022;265:126258.

[3] Mamat R, Sani M, Sudhakar K, Kadarohman A, Sardjono R. An overview of Higher alcohol and biodiesel as alternative fuels in engines. Energy Rep 2019;5:467–79.

[4] Fayad MA, Tsolakis A, Martos FJ. Influence of alternative fuels on combustion and characteristics of particulate matter morphology in a compression ignition diesel engine. Renew Energy 2020;149:962–9.

[5] Sharma S, Sharma D, Soni SL, Singh D, Jhalani A. Performance, combustion and emission analysis of internal combustion engines fuelled with acetylene–a review. Int J Ambient Energy 2022;43(1):622–40.

[6] Uludamar E, Tosun E, Tüccar G, Yıldızhan Ş, Çalık A, Yıldırım S, et al. Evaluation of vibration characteristics of a hydroxyl (HHO) gas generator installed diesel engine fuelled with different diesel–biodiesel blends. Int J Hydrogen Energy 2017;42(36):23352–60.

[7] Ozcanli M, Akar MA, Calik A, Serin H. Using HHO (Hydroxy) and hydrogen enriched castor oil biodiesel in compression ignition engine. Int J Hydrogen Energy 2017;42(36):23366–72.

[8] Kenanoğlu R, Baltacıoğlu MK, Demir MH, Özdemir ME. Performance & emission analysis of HHO enriched dual-fuelled diesel engine with artificial neural network prediction approaches. Int J Hydrogen Energy 2020;45(49):26357–69.

[9] Baltacioglu MK, Kenanoglu R, Aydın K. HHO enrichment of bio-diesohol fuel blends in a single cylinder diesel engine. Int J Hydrogen Energy 2019;44(34):18993–9004.

[10] Rajaram PS, Kandasamy A, Remigious PA. Effectiveness of oxygen-enriched hydrogen-hho gas addition on direct injection diesel engine performance, emission and combustion characteristics. Therm Sci 2014;18(1):259–68.

[11] Thangaraj S, Govindan N. Evaluating combustion, performance and emission characteristics of diesel engine using Karanja oil methyl ester biodiesel blends enriched with HHO gas. Int J Hydrogen Energy 2018;43(12):6443–55.

[12] Manu P, Sunil A, Jayaraj S. Experimental investigation using an on-board dry cell electrolyzer in a CI engine working on dual fuel mode. Energy Procedia 2016;90:209–16.

[13] Arjun T, Atul K, Muraleedharan AP, Walton PA, Bijinraj P, Raj AA. A review on analysis of HHO gas in IC engines. Mater Today: Proc 2019;11:1117–29.

[14] Nabil T, Dawood MMK. Enabling efficient use of oxy-hydrogen gas (HHO) in selected engineering applications; transportation and sustainable power generation. J Clean Prod 2019;237:117798.

[15] Yilmaz AC, Uludamar E, Aydin K. Effect of hydroxy (HHO) gas addition on performance and exhaust emissions in compression ignition engines. Int J Hydrogen Energy 2010;35:11366–72.

[16] Bahmanyar D, Razmjooy N, Mirjalili S. Multi-objective scheduling of IoT-enabled smart homes for energy management based on Arithmetic Optimization Algorithm: A Node-RED and NodeMCU module-based technique. Knowl-Based Syst 2022;247:108762.

[17] Alferaidi A, Yadav K, Alharbi Y, Razmjooy N, Viriyasitavat W, Gulati K, et al. Distributed deep CNN-LSTM model for intrusion detection method in IoT-based vehicles. Math Probl Eng 2022;2022.

[18] Arat HT, Baltacioglu MK, Özcanli M, Aydin K. Effect of using Hydroxy – CNG fuel mixtures in a non-modified diesel engine by substitution of diesel fuel. Int J Hydrogen Energy 2016;41(19):8354–63.

[19] El-Kassaby MM, Eldrainy YA, Khidr ME, Khidr KI. Effect of hydroxy (HHO) gas addition on gasoline engine performance and emissions. Alex Eng J 2016;55(1):243–51.

[20] Gohar GA, Raza H. Comparative analysis of performance characteristics of CI engine with and without HHO gas (Brown gas). Advances in Automobile Engineering 2017;6(172):2.

[21] Matienzo JMR. Influence of addition of hydrogen produced on board in the performance of a stationary diesel engine. Int J Hydrogen Energy 2018;43(37):17889–97.

[22] Rimkus A, Matijošius J, Bogdevičius M, Bereczky Á, Török Á. An investigation of the efficiency of using O_2 and H_2 (hydrooxile gas -HHO) gas additives in a ci engine operating on diesel fuel and biodiesel. Energy 2018;152:640–51.

[23] Nabil T. Efficient Use of oxy-hydrogen gas (HHO) in vehicle engines. Int Inform Eng Technol Assoc 2019;1:87–96.

[24] Kazim AH, Khan MB, Nazir R, Shabbir A, Abbasi MS, Abdul Rab H, et al. Effects of oxyhydrogen gas induction on the performance of a small-capacity diesel engine. Sci Prog 2020;103(2). 0036850420921685.

[25] Najafi B, Haghighatshoar F, Ardabili S, Band SS, Chau KW, Mosavi A. Effects of low-level hydroxy as a gaseous additive on performance and emission characteristics of a dual fuel diesel engine fueled by diesel/biodiesel blends. Eng Appl Comput Fluid Mech 2021;15(1):236–50.

[26] Dahake M, Patil S, Malkhede D. Experimental investigation of performance and emissions of single-cylinder diesel engine enriched by hydroxy gas for various compression ratios. In: *Advances in Mechanical Processing and Design*. Springer; 2021. p. 127–38.

[27] Dahake MR, Patil SD, Patil SE. Effect of hydroxy gas addition on performance and emissions of diesel engine. Int Res J Eng Technol 2016;3(1):756–60.

[28] Al-Dawody MF, Jazie AA, Abbas HA. Experimental and simulation study for the effect of waste cooking oil methyl ester blended with diesel fuel on the performance and emissions of diesel engine. Alex Eng J 2019;58:9–17.

[29] Kuleshov AS. Model for predicting air-fuel mixing, combustion and emissions in DI diesel engines over whole operating range. *SAE Technical Paper* 2005-01-2119; 2005. Doi: 10.4271/2005-01-2119.

[30] Kuleshov A, Mahkamov K. Multi-zone diesel fuel spray combustion model for the simulation of a diesel engine running on biofuel. Proc Inst Mech Eng, Part A: J Power Energy 2008;222:309–21.

[31] Al-Dawody MF. Theoretical study for the influence of biodiesel addition on the combustion, performance and emissions parameters of single cylinder diesel engine. J Univ Babylon 2017;25:1830–9.

[32] Al-Dawody MF, Bhatti S. Optimization strategies to reduce the biodiesel NOx effect in diesel engine with experimental verification. Energ Conver Manage 2013;68:96–104.

[33] Al-Dawody MF, Bhatti S. Effect of variable compression ratio on the combustion, performance and emission parameters of a diesel engine fuelled with diesel and soybean biodiesel blending. World Appl Sci J 2014;30:1852–8.

[34] Alkidas AC. Relationships between smoke measurements and particulate measurements. Warrendale, PA: Society of Automotive Engineers Inc; 1984.

[35] Masjuki H, Ruhul A, Mustafi NN, Kalam M, Arbab M, Fattah IR. Study of production optimization and effect of hydroxyl gas on a CI engine performance and emission fueled with biodiesel blends. Int J Hydrogen Energy 2016;41:14519–28.

[36] Talibi M, Hellier P, Balachandran R, Ladommatos N. Effect of hydrogen-diesel fuel co-combustion on exhaust emissions with verification using an inecylinder gas sampling technique. Int J Hydrogen Energy 2014;39(27):15088–102.

[37] Ma F, Wang M, Jiang L, Deng J, Chen R, Naeve N, et al. Performance and emission characteristics of a turbocharged spark-ignition hydrogen-enriched compressed natural gas engine under wide open throttle operating conditions. Int J Hydrogen Energy 2010;35:12502–9.

[38] S. N, Nagarajan G, Dhanasekaran C, et al. Experimental investigation of hydrogen port fuel injection in DI diesel engine, *Int J Hydrogen Energy* 2007;32:4071–80.

[39] Szwaja S, Grab-Rogalinski K. Hydrogen combustion in a compression ignition diesel engine. Int J Hydrogen Energy 2009;34:4413–21.

[40] Bari S, Esmaeil MM. Effect of H_2/O_2 addition in increasing the thermal efficiency of a diesel engine. Fuel 2010;89:378–83.

[41] Wang S, Ji C, Zhang J, Zhang B. Comparison of the performance of a spark-ignited gasoline engine blended with hydrogen and hydrogen–oxygen mixtures. Energy 2011;36:5832–7.

[42] Wang S, Ji C, Zhang J, Zhang B. Improving the performance of a gasoline engine with the addition of hydrogen–oxygen mixtures. Int J Hydrogen Energy 2011;36:11164–73.

[43] Ji C, Wang S. Experimental study on combustion and emissions performance of a hybrid hydrogen–gasoline engine at lean burn limits. Int J Hydrogen Energy 2010;35:1453–62.

[44] Varde KS, Frame GA. Hydrogen aspiration in direct injection type diesel engine-its effect on smoke and other engine performance parameters. Int J Hydrogen Energy 1983;8:549–55.

[45] Karago Y, Tarkan Sandalc, Levent Yüksek, Ahmet Selim Dalkılıcx and Somchai Wongwises. Effect of hydrogen–diesel dual-fuel usage on performance, emissions and diesel combustion in diesel engines. *Adv Mech Eng* 2016;8:1–13.